7-9-2009

Palmitic Acid Increases Enac Expression and Contributes to Insulin Resistance in Renal Distal Tubule

Timmy Sullivan

PALMITIC ACID INCREASES ENAC EXPRESSION AND CONTRIBUTES TO INSULIN RESISTANCE IN RENAL DISTAL TUBULE

A Thesis Submitted to the
Yale University School of Medicine
In Partial Fulfillment of the Requirements for the
Degree of Doctor of Medicine

By
Timmy Sullivan
2008

ABSTRACT

Insulin resistance and obesity are two conditions associated with hypertension. Although the causes of hypertension are likely to be multifactorial, dysregulation of renal distal tubule sodium reabsorption may play a role. It has been shown that insulin increases sodium reabsorption in the distal tubule through the increased expression of epithelial sodium channels (ENaC); and obesity has been shown to cause insulin resistance in various tissues. Thiazolidinediones (TZDs) are insulin-sensitizing drugs whose use can be limited by a side effect of fluid-retention leading to edema and congestive heart failure. We set out to determine if the expression of ENaC in distal tubule cells, as modeled by the A6 (frog nephron) cells, became resistant to insulin following exposure to various concentrations of free-fatty acids (FFAs). We then set out to determine if TZDs had an insulin-sensitizing effect on distal tubule cells in both a FFA naive environment and after being exposed to FFAs. We exposed monolayers of A6 nephron cells to palmitic acid (PA) in concentrations of 0, 0.25, 0.5, 1, and 1.5 mM. After an incubation time of 20 hours we stimulated the cells with insulin. Measuring the cells with equivalent short-circuit current we found that as the PA concentration increased from 0 to 0.5 mM there was an increase in current (Isc), implying an increase in ENaC activity, followed by a marked decrease in Isc at PA concentrations of 1 mM or greater. Consistent with an increase in Isc, the calculated transepithelial resistance decreased with 0.25 and 0.5 mM PA, however, at higher concentrations of PA we observed a marked drop in resistance, implying probable apoptosis. After insulin treatment we found that in control cells (0 mM PA) the Isc increased 100% whereas with increasing concentrations of PA, there was

a smaller fractional increase of 46%, 12% and 0% at 0.25, 0.5 and 1.0 mM PA, respectively. After verifying that PPARα, β, and γ were expressed in these cells we treated A6 cells with 10 μM of Rosiglitazone (PPARg agonist) or 3 mM of Clofibrate (PPARa agonist). We found there was no change in Isc following exposure to these drugs. We next pretreated the cells with both 0.5 mM PA with Clofibrate or Rosiglitazone. Again, there was no statistically-significant difference between these conditions. Overall we found that exposure to PA caused resistance to the insulin induced ENaC expression in A6 cells; at small concentrations of PA there was increased base-line ENaC expression but higher concentrations were toxic to the cells. We also found that TZDs did not have any effect on ENaC expression at base-line, with insulin, or with exposure to PA.

INTRODUCTION

ENaC

Epithelial Na+ channels (ENaC) are located on the apical face of many sodium-absorbing epithelia. They facilitate the passive transport of Na+ into these cells as the initial step in transporting the Na+ through the epithelia. The passive transport is driven by the Na+/K+-ATPase located on the basolateral side of the cells ({{175 Garty,H. 1997; }}). ENaC is composed of three homologous subunits: α, β, and γ; and is a tetrameric channel with an $\alpha_2\beta\gamma$ stoichiometry ({{176 Kosari,F. 1998; }}). Regulation of ENaC can be achieved, pharmacologically, with amiloride, which blocks the channel completely; and, depending on the tissue, ENaC activity can be increased with the hormones aldosterone, vasopressin, or insulin.

ENaC is found in a wide variety of epithelial cells: the kidney, bladder, intestines, sweat and salivary glands, lung, taste cells, mechanosensory cells, and in amphibian skin among others. Though the physiologic purpose of ENaC varies from tissue to tissue, the function of the channel remains the same: passive absorption of Na+.

ENaC in the distal convoluted tubule

The kidney plays a crucial role in fluid and electrolyte homeostasis. Total body Na+ concentration is the main determinant of extra-cellular fluid volume. The filtered load of Na+ in human kidneys is approximately 25,500 mmole/day, or 1.5 kg of table salt or

about 9 times the total amount of Na+ present in the body{{178 Boron, Walter F. 2003; }}; therefore, since the kidney filters the entire vascular fluid many times a day, it is crucial that almost all the Na+ is reabsorbed. 65% of the filtered sodium load is reabsorbed in the proximal tubule, 25% is reabsorbed in the thick ascending limb, and the remaining 10% is reabsorbed distal to the macula densa. This distal portion of the nephron is broken down into the distal convoluted tubule, the cortical collecting tubule, and the medullary collecting duct. The principal cells of the cortical collecting tubule and collecting duct absorb Na+ via ENaC; and although Na+ absorption in this portion of the nephron only accounts for around 2-3% of the filtered Na+ load, it is crucial to extra-cellular fluid volume status. This is illustrated by the results of two disorders that manifest themselves through dysfunctions of ENaC regulation in the distal tubule.

In Liddle's syndrome ENaC activity and/or expression is constitutively increased leading to severe hypertension that is refractory to treatment except from ENaC blockers. In pseudohypoaldosteronism type 1 a defect in one or more of the ENaC sub-units which prevents their insertion into the apical cell membrane leads to excess fluid and Na+ excretion in the urine leading to salt wasting, hyperkalaemia, and metabolic acidosis, despite increased serum aldosterone levels.

Regulation

ENaC activity in the distal tubule is regulated by the renin-angiotensin-aldosterone axis (RAA), arginine vasopressin (AVP) or anti-diuretic hormone (ADH), insulin, the sympathetic nervous system, and atrial natriuretic peptide (ANP). RAA, AVP/ADH, and

the sympathetic nervous system increases Na+ retention in response to decreased vascular pressure. ANP atrial natriuretic peptide increases Na+ excretion in response to an overly distended right atrium. Aldosterone acts to increase the transcription, translation, and number of ENaC channels present on the apical side of the cells which leads to increased Na+ absorption{{172 Alvarez de la Rosa,D. 2002; }}.

Insulin also increases Na+ retention in both the thick ascending limb and the distal nephron, particularly the cortical nephron. Similar to aldosterone, insulin increases the density of ENaC channels present on the apical side of the distal tubule. Though both hormones increase the number of channels, they act through two different mechanisms over different time periods; aldosterone induces new protein production and increases channel density over a period of hours; whereas insulin increases channel density within minutes. It has been postulated that insulin initiates fusion between the apical cell membrane and pre-formed intra-cellular vesicles containing ENaC channels. Though both hormones have the same general effect, they appear to work through independent mechanisms {{179 Blazer-Yost,B.L. 1998; }}.

ENaC in Xenopus l.: A good model for mammalian dct and ENaC

ENaC is also found in a model renal-like epithelia cell line called A6 derived from the frog kidney of Xenopus laevis. This cell line provided the cells in which we conducted our experiments. A6 epithelia are a widely used model for mammalian distal tubule; in a paper by Shane et al, this A6 cell line was compared to mouse principal cells of the kidney cortical collecting duct and were shown to have similar responses to aldosterone,

insulin, vasopressin, and amilioride{{177 Shane,M.A. 2006; }}. Other advantages to this cell line are that it provides homologous ENaC genotypes and phenotypes, and that it is a single cell type.

INSULIN

Insulin is a secretory protein synthesized in the β cells of the pancreas. In a healthy individual the secretion of insulin is closely linked to rising blood-glucose levels and is the major hormone responsible for coordinating the body's fuel metabolism. Insulin has profound effects on both carbohydrate and lipid metabolism and significant influence on protein and mineral metabolism.

Insulin affects many tissues. Generally considered "the well-fed hormone" because of its increased secretion following food intake, insulin manages the body's reaction to absorbed glucose. In the liver, the increased plasma insulin promotes formation of glycogen from glucose, promotes lipogenisis, the formation of triglycerides, and decreases the breakdown of glycogen. In both adipose and muscle tissue, insulin acts to increase the oxidation of carbohydrates as a principle fuel source, while converting the excess glucose present in the bloodstream into lipids or glycogen. Insulin receptors are found in many tissues; however Shulman et al showed that muscle plays the greatest role in insulin and glucose homeostasis and is a thoroughly studied area{{180 Shulman,G.I. 1990; }}. As we already noted, the distal tubule is also sensitive to insulin. Though not a

major factor in glucose homeostasis, insulin acts to increase ENaC expression on the apical side of the tubule cells.

Insulin resistance and hyper-insulinemia

Though many tissues are sensitive to insulin, some tissue can become resistant to insulin. Insulin resistance is simply a condition where a given concentration of insulin produces a less-than-expected biological effect and comprises a broad spectrum of disorders including diabetes, syndrome X, obesity, and glucose intolerance{{181 Olatunbosun, S.T.; }}. The significance of these conditions is immense. Type 2 diabetes alone is the leading cause of blindness among working-age adults, end-stage renal disease, and non-traumatic loss of limb, and the 5th leading cause of death in the U.S.. Financially, the costs of type 2 diabetes is $92 billion in the U.S. alone {{182 Petersen,K.F. 2006; }}.

The cause of insulin resistance has not been fully elucidated. Once again research into muscle's role in insulin/glucose homeostasis gives us the most information on possible mechanisms. As glucose is taken up from the bloodstream, muscle cells convert the glucose to glycogen through a series of biochemical steps. It has been shown that insulin resistance in muscle is attributed to a reduction in insulin-stimulated glucose transport into the cells and not an induced dysfunction down-stream in the glycogen pathway {{182 Petersen,K.F. 2006; }}.

One cause of insulin resistance in muscle appears to be intracellular lipid content. It has been shown that there is a negative correlation between intracellular triglyceride (TG)

content and glycogen synthase activity; it was also shown that there was a positive correlation between intracellular lipid content and features of insulin resistant syndromes such as: increased waist to hip ratio, and fasting nonesterified fatty acid levels{{183 Phillips,D.I. 1996; }}. It has also been shown that children of parents with type 2 diabetes are 40% more likely to get it than controls and that the increased concentration of plasma fatty acids in these individuals is significantly correlated with their insulin resistance{{184 Perseghin,G. 1997; }}.

Not all the tissue types that are sensitive to insulin become insulin resistant at the same rate. Some of the problems encountered in insulin resistant states are a result of certain tissue not becoming resistant to the effects of insulin. For example, in a patient whose muscle tissue requires a higher concentration of insulin for normal glucose homeostasis, the hyperinsulinemia acting on the liver, which is not initially as resistant to the effects of insulin, leads to hypertriglyceridemia; and on the ovary it leads to hyperandrogenism. In studies of the kidneys, rats, rabbits, and anecdotal evidence concerning humans indicate that chronic insulin infusion or hyperinsulinemia leads to increased ENaC expression and Na+ retention in the distal tubule. This increased retention of Na+ and the resultant intra-vascular volume expansion is one possible etiology of hypertension (HTN) in the hyperinsulinemic state{{186 Baum,M. 1987; }}{{188 Song,J. 2006; }}.

HYPERTENSION

Hypertension (HTN) in an otherwise healthy adult is defined as a systolic and/or diastolic arterial pressure greater than 140 and 90 mm Hg respectively. Worldwide the prevalence of HTN may be as high as 1 billion with approximately 7.1 million deaths attributable to it each year {{189 Chobanian,A.V. 2003; }}. The World Health Organization estimates HTN is responsible for 62% of cerebrovascular disease and 49% of ischemic heart disease and is the number one attributable risk for death in the world{{189 Chobanian,A.V. 2003; }}. The etiology of hypertension is multifactorial and very complex. Aspects of the circulating blood volume such as viscosity, vascular reactivity, humoral mediators, cardiac output, neural stimulation, and others, including increased sodium retention contribute to HTN.

The Role of ENac in HTN

Since total body sodium determines the extra-cellular fluid volume, pathologic up-regulation of sodium re-absorption in the kidney can lead to HTN{{163 Herlitz,H. 1996; }}. As sodium intake changes throughout the day, the distal nephron responds by altering the amount of sodium absorbed from the lumen of the tubule. ENaC inserted in the apical side of the cells are responsible for this re-absorption{{164 Horisberge, J.D. 1993; }}{{165 Barbry,P. 1997; }}. ENaC expression and activity is up-regulated in response to low blood pressure, but in a pathologic state ENaC activity can be increased by various mechanisms, regardless of blood pressure, leading to HTN{{166 Ecelbarger,C.A. 2006; }}. An extreme example of this pathology is illustrated by Liddle's syndrome which is a disease resulting from increased ENaC activity leading to hypokalemia, metabolic alkalosis, and HTN{{173 Hummler,E. 2003; }}. Lending

credence to the observation that ENaC is responsible for the HTN in Liddle's syndrome is the therapy employed to deal with the disease which consists of amiloride and triamterene both of which directly block ENaC; and spironolactone, a mineralocorticoid antagonist, is ineffective at treating this disorder{{190 Botero-Velez,M. 1994; }}.

FREE FATTY ACIDS

Fatty acids are the main source of reserve energy in the body. Most fatty acids are supplied by the diet but they can also be synthesized de novo from excess carbohydrates and protein. Fatty acids in the circulation, either bound to albumin or not, are referred to as 'free fatty acids' (FFAs). The normal serum concentration of FFAs is between 200-600 μM{{195 Synak,M. 2003; }} and generally consists of a mixture of 6 FFAs: palmitate (25%), stearate (10%), oleate (38%), linoleate (22%), arachidonate (3%), and linolenate (2%){{199 Azzazy,H.M. 2006; }}. Although serum concentrations run between 200 and 600 μM, FFAs aggregate at concentrations as low as 5-10 μM in an aqueous solution; therefore almost all free fatty acids are transported in a complex with albumin. Almost all of the FFAs in serum are transported in this way with <0.01% free in solution {{196 Richieri,G.V. 1995; }}.

Free-Fatty-Acids and Insulin Resistance

As stated earlier, an elevated serum concentration of FFAs has been shown to be an independent risk factor for HTN, insulin resistance, and hyperglycemia{{197 Fagot-

Campagna,A. 1998; }}{{198 Griffin,M.E. 1999; }}. FFAs inhibit insulin stimulated glucose transport in a dose dependent fashion through multiple mechanisms such as: defects in glucose uptake, defects in proper phosphorylation, and inhibition of glycogen synthase{{200 Boden,G. 1998; }}. Excess FFAs contribute to hyperglycemia by both inducing insulin resistance and by increasing hepatic glucose production. Though beneficial in the conditions of starvation or pregnancy, FFA induced insulin resistance in a well-fed state can lead to multiple morbidities.

PPARs

Peroxisome proliferators-activated receptors (PPARs) are ligand-activated transcription factors and members of the nuclear hormone receptor family. PPARs exist in three isoforms: PPARα, PPARδ, and PPARγ. PPARs were originally named for their ability to induce hepatic peroxisome proliferation in mice in response to xenobiotic stimuli {{201 Semple,R.K. 2006; }}. Studies have suggested these receptors are involved in lipid regulation, metabolism, and nutrient sensing {{201 Semple,R.K. 2006; }}. PPARα binds to fibrates such as clofibrate and natural ligands such as leukotriene B4 and is a key regulator of lipid oxidation and has some effects on insulin sensitivity. PPARδ appears to play a role in fatty-acid controlled differentiation of preadipose cells{{203 Bastie,C. 2000; }}. PPARγ binding with its insulin-sensitizing ligands, thiazolidinediones (TZDs), lowers glucose levels and FFA levels{{202 Takahashi,S. 2006; }}. Besides the agonist

mentioned specifically for each moiety of PPAR, saturated and unsaturated fatty acids also act as ligands to this family of receptors{{202 Takahashi,S. 2006; }}.

PPARs and ENaC

It was established that there is a high expression of PPARγ in the inner medullary collecting ducts of both rabbits and humans, with some expression of PPARα{{204 Guan,Y. 1997; }}. Studies are conflicted concerning the effects of PPARγ activation in the DCT. They have shown that PPARγ agonists both increase the basal and insulin stimulated Na+ flux via ENaC in the distal tubule and that PPARγ agonists have no effect at all{{205 Nofziger,C. 2005;206 Guan,Y. 2005; }}. Since TZDs both increases the body's sensitivity to insulin and reduces the serum triglyceride and FFAs levels, they are increasingly used in the treatment of type 2 diabetes mellitus. However 10-15% of patients using TZDs are forced to discontinue usage because of dependent edema and congestive heart failure{{207 King,K.A. 2004; }}. Because these drugs are so effective in treating type 2 diabetes, it is important to determine the true cause of these side effects from TZDs.

HYPERTENSION, INSULIN RESISTANCE, FFAs, and THE GOALS OF OUR STUDY

Hypertension (HTN), insulin resistance, and obesity are three of the core components of metabolic syndrome{{155 Ford,E.S. 2002; }}. Although criteria defining the syndrome

have changed through the years, these three aspects of the syndrome have been used consistently to diagnose the disorder. Affecting approximately 22 percent of Americans with a prevalence increasing to almost 45 percent by the ages of 60-69{{155 Ford,E.S. 2002; }}, the syndrome dramatically raises the risk for many conditions, including: type 2 diabetes, cardiovascular disease{{156 Wong,J. 2006; }}, chronic kidney disease, cognitive decline, dementia{{157 Roriz-Cruz,M. 2006; }}, and many other pathologic states.

The link between these three conditions is complex and not fully elucidated. There is evidence that increased concentrations of free-fatty acids (FFAs) in the blood are toxic to pancreatic β-cells, leading to type-2 diabetes{{158 Karaskov,E. 2006; }}. There are also proposed mechanisms in which type-2 diabetes leads to increased FFAs{{161 Garvey,W.T. 2003; }}. Both conditions can lead to HTN through multiple pathways{{162 Boden,G. 2006; }}. One of these mechanisms is an alteration of sodium homeostasis. Since total body sodium determines the extra-cellular fluid volume and therefore a major component of blood pressure, pathologic up-regulation of sodium re-absorption in the kidney can lead to HTN{{163 Herlitz,H. 1996; }}.

The interplay between insulin resistance, dyslipidemia, and hypertension as seen in metabolic syndrome led us to investigate two possible etiologies for HTN in insulin resistant states. As stated earlier, distal tubule cells respond to insulin by increasing expression of ENaC {{167 Asher,C. 1996; }}and many tissues become insulin resistant following exposure to increased serum FFAs, but, once again, not all tissues becomes

insulin resistant at the same rate. Therefore, we postulated that if distal tubule cells remain sensitive to insulin following exposure to FFAs, the increased serum insulin found in insulin resistance could lead to increased ENaC expression in the distal tubule, leading to increased Na+ uptake, volume expansion, and finally result in HTN.

Secondly, if distal tubule cells did become insulin resistant following exposure to FFAs, we set out to determine a possible mechanism for the observed increase in ENaC expression in dyslipidemic and hyperinsulinemic states. Since some studies claim that TZD-induced insulin sensitivity can lead to up-regulation of ENaC in the distal tubule resulting in edema, and possibly HTN, and because FFAs have been shown to be agonists for PPARs, we compared the response of Xenopus laevis A6 cells exposed to increased concentrations of the FFA palmitate to the cells same response to various PPAR agonists. If the mechanism through which pathologic ENaC up-regulation in a diseased state occurs can be determined it would provide a valuable target for HTN therapy in an insulin resistant individual.

METHODS

Cell Culture

A6 cells derived from the kidney of *Xenopus laevis* were provided by Dr. John Hayslett (Yale University, New Haven, CT)(7 Hayslett,J.P. 1995). Cells were maintained in amphibian medium in an incubator set at 27°C and with 1.5% CO_2. All experiments were performed with passages between 105 and 115. Cells were expanded on 100 mm plastic dishes (Corning®). The cells were grown until confluent and then seeded on 6.5 mm permeable supports (Transwell® polycarbonate membrane with a pore size of 0.4 μm; Costar). 250 μL of medium was added to the inner well and 800 μL was added to the outer well. Medium was changed every 4-5 days. Once the cells showed stable current and voltage, usually 8-10 days after seeding on transwells, the growing medium was replaced with serum-free medium and aldosterone was added to a final concentration of 100 nM. The cells were then placed back in the incubator to stabilize. After 12 hours the current and voltage were measured to determine a baseline. At this point we began our experiments.

Preparing Amphibian Medium

The medium in which the cells were maintained was made by adding 3 packages of Dulbecco's Modified Eagle Medium 10g (powder, low glucose, with L-glutamine, sodium pyruvate, and pyridoxine hydrochloride, without sodium bicarbonate, Gibco BRL Life Technologies cat. # 31600-034) to 3600 ml of deionized water. 3.85 g $NaHCO_3$ was added and equilibrated with 1.5% CO_2 to attain pH 7.4. 10 ml L-Glutamine (Gibco

200mM – 100x solution, cat. # 25030-081) was then added. Fetal bovine serum (FBS) (Gibco BRL Life Technologies, cat. #26140-079) was first heat-inactivated for 30 minutes at 56°C and added to be 10% of the final volume in the medium. Penicillin and streptomycin were added for a concentration of 1% of the final volume.

Fatty Acid

Various concentrations of Palmitic acid (PA) (Sigma-Ultra, cat. # 5585) ethanol, amphibian medium, and bovine serum albumin (BSA) (American Bioanylytical, cat. # AB00440) were used for these experiments. A 0.2 M stock solution was prepared by dissolving PA in ethanol and filtering into a sterile container. BSA was added to amphibian medium without FBS to a final concentration of 20%, gently agitated until dissolved, and filtered into a separate sterile container. PA working solution was added to the BSA/amphibian medium to prepare concentrations of 0.25, 0.5, 1, and 1.5 mM. These solutions were agitated at a high rate at 37º using an Environshaker (Lab-line) for 6-8 hours. Aldosterone was added to each solution for a final concentration of 100 nM/ml. Solutions were filtered through 0.2 μm filters and added directly to the cells.

PPAR agonist

When indicated cells were treated with the PPARγ agonist Rosiglitazone (Cayman Chemical Co., cat. # 71740) to a final concentration of 10 μM or treated with PPARα agonist Clofibrate (Sigma-Aldrich cat. # 6643) to a final concentration of 3 mM. Twenty hours after addition of the drugs, measurements of Isc, transepithelial voltage and resistance were obtained.

Equivalent Short-circuit Current Measurements

After 20-24 hours of exposure to the experimental conditions voltage and current across confluent monolayers of A6 cells were measured with $Ag/AgCl_2$ electrodes (made at Yale electronics shop) connected to a DVC-1000 voltage/current-clamp apparatus (World Precision Instruments). Short circuit current was measured while the transepithelial voltage was clamped at 0 mV and at –20 mV. Transepithelial resistance was calculated from the change in current induced by 20 mV change in voltage according to Ohm's law.

Western Blotting

Following the electrophysiological measurements the medium containing lipids was aspirated and the filters were washed with PBS. The filters were removed from the supports and placed in separate microfuge tubes with 30µl of solubilization buffer (in mM: 100 NaCl, 50 Tris, pH 8.0, and 1% TritonX-100). Nonsoluble material was removed by centrifugation at 14,000 rpm for 5-10 minutes. The supernatant was recovered and used in the Western blotting. After separation in 10% SDS-PAGE gels, proteins were transferred to Immobilon-P membranes (Millipore). Membranes were blocked with 5% fat free milk in (mM): 100 NaCl, 50 Tris, pH 8.0, and 0.1% Tween. ENaC subunits were detected by Western blotting with affinity purified anti-*x*ENaC antibodies at 1:8,000 dilution were added and incubated for 1 h on a rocking platform. Actin was detected with a commercially available antibody (mouse monoclonal antiactin antibody, Chemicon International). After three washes of 15 min the membranes were incubated with anti–mouse or anti-rabbit IgG antibodies conjugated to peroxidase (Sigma-Aldrich) at

1:10,000 dilution. After washes the signal was developed with the ECL+ system (Amersham Pharmacia Biotech).

Immunofluorescence

Cells on filters were fixed with 4% paraformaldehyde fin PBS for 30 min at RT. Cells were washed in PBS, permeabilized with 1% TritonX-100 for 20 min. Phalloidin conjugated with Texas red (1:500 dilution) was added to cells for 1 h. Cells were washed three times for 15 min with PBS. Filters were removed from support with a fine scalpel and mounted on slides overlay with mounting solution (VectaShield) supplemented with DAPI. Filters were examined under a fluorescent microscope Axiophot (Zeiss).

Staining with Oil Red O

A stock solution of Oil Red O was prepared from 0.5 g of Oil Red O in 100 mL of isopropanol. The working solution consisted of 30 mL of the stock solution added to 20 mL distilled water and filtered. Cells on filters were fixed with 4% paraformaldehyde in PBS for 30 min at RT. Cells were washed in PBS and then rinsed with 60% isopropanol, then stained with Oil Red O working solution for 15 minutes and rinsed again with 60% isopropanol. The cells were then lightly stained with haematoxylin for 1 minute and rinsed with distilled water. Filters were removed from support with a fine scalpel and mounted on slides overlay with mounting solution (VectaShield) and examined under a light microscope.

Northern Blot Analysis.

Isolation of RNA. A6 cells were grown on 24 mm diameter filters for 10 days. Cells were exposed to PA at the indicated concentrations for 20 h. Total RNA was extracted using RNeasy Mini Kit (Qiagen). Concentration of RNA was calculated by OD measurement at 260 and 280 nm

Electrophoresis of RNA. 10 μg of RNA in 5.5 μl from each condition was mixed with 5.4 μl 6 M glyoxal, 16 μl of DMSO, 3 μl of 0.1 M sodium phosphate and 4 μl of loading buffer. The RNA was resolved in 1% agarose gel in 10 mM $NaPO_4$ buffer. RNA was transferred to nylon membrane (Amersham) by capillary elution on 20 SSC (3 M NaCl; 0.3 M Na-citrate) for 20 h.

Preparation of radioactive probes. 50 ng of DNA corresponding to the coding sequence of α, β, and γ ENaC subunits and α subunit of the Na/K-ATPase were used with Random Primed DNA Labeling kit (Roche). For each probe the reaction consisted of: 25 ng DNA in 9 μl of water denatured by heating at 95^{o}C for 10 min, 3 μl of dNTP mix minus dCTP, 2 μl of reaction mixture containing random primers, 5 μl of 50 μCi [α-^{32}P]dCTP, and 1 μl of Klenow enzyme. The reactions were incubated at 30^{o}C for 1 h and stopped by heating at 65^{o}C for 10 min. Unincorporated deoxyribonucleoside triphosphates were removed with Quick Spin Column, Sephadex G-50.

Hybridization of probes. Prior to hybridization RNA was cross-linked to nylon membrane by UV light 254 nm using Stratalinker and auto crosslink setting. Pre hybridization consisted of 5 x SSC; 50 % Formamide; 5 x Denhardt's-solution; 1 % SDS; 100 μg/ml heat-denatured sheared salmon sperm DNA. Probes were denatured and immediately mixed with pre-hybridization solution. Membranes were incubated at 42^{o}C

for 12 h. Membranes were subsequently washed 1 x 15 min with 2 x SSC @ RT followed by wash with 2 x SSC, 0.1 % SDS @ 65 °C until background was low. Membranes were covered with saran wrap and exposed to film with intensifying screen at -80°C.

Composition of 100 x Denhardt's-solution (500 ml): 10 g Ficoll 400; 10 g polyvinylpyrrolidone MW 360000; 10 g BSA fraction V; H_2O.

RESULTS

Short-circuit Current Examination of A6 Cells

In order to examine ENaC activity after exposure to free-fatty acids (FFAs) we used cells derived from the distal tubule of *Xenopus laevis* (A6). Sodium from the lumen enters the cell via ENaC driven by a favorable electrochemical potential and exits at the basolateral side by the Na-K/ATPase. This process generates a current that can be measured using the method of short-circuit current. Isc is a valid measurement of ENaC activity because in A6 cells almost 100% of the transepithelial current is generated by sodium transport through ENaC{{172 Alvarez de la Rosa,D. 2002; }}. Another advantage of A6 cells is that they form monolayers with tight junctions that exhibit high electrical resistance thereby changes in resistance can be used to monitor the health of the monolayer.

A6 Cells response to Insulin and Aldosterone

A6 cells respond to insulin and aldosterone by increasing ENaC activity. After exposure to insulin A6 cells increase ENaC activity; the response is quick acting (~3 min) reaching a plateau at ~30 min{{172 Alvarez de la Rosa,D. 2002; }}. This time course suggests that intra-cellular vesicles containing pre-assembled ENaC channels merge with the apical membrane. Such a mechanism is reminiscent of insulin-stimulated translocation of GLUT4 in skeletal muscle, a process that is blunted when FFAs are elevated{{31 Yu,C. 2002; }}. For this reason we exposed the cells to insulin at the end of 20 hours of PA treatment and re-measured Isc 30 min later. Unlike insulin, aldosterone increases transcription of ENaC and therefore takes much longer, over 6 hours, to reach a maximal

effect{{172 Alvarez de la Rosa,D. 2002; }}. Since there are more channels available with aldosterone, the over-all current and voltage increase. It was necessary to have a large magnitude of Isc in order to detect changes induced by PA.

Growth Mediums

The medium to grow A6 cells had to be modified because these are amphibian-derived cells that require 190 mOsm. In addition, cells were grown in an incubator set at 29°C and [CO_2] of 1.5% to mimic the conditions of amphibian cells. Cells were bathed in a serum-rich medium until they showed significant voltage and current resistance, implying they were both healthy and confluent across the filter. Cells were switched to serum-free medium for 12 hours before beginning experiments to remove lipids contained in the serum.

Palmitic Acid

Because it is the one of the most abundant saturated free-fatty acid present in the body we chose to use palmitic acid for our experiments. We prepared concentrations of 0, 0.25, 0.5, 1, and 1.5 mM PA. The physiologic concentrations of FFAs in a non-diseased state range from 200 to 600 μM, and from 400 to 2000 μM in insulin resistant states with PA making up approximately 25% of that total. From previous trials (not shown) we determined an optimal time-course to conduct the experiments. We saw effects beginning at 6 hrs, but a peak effect at 18-24 hours, so we chose to incubate the cells in the PA solution for ~20 hours.

Effects of Increasing Concentrations of PA on Current, Voltage, Resistance, and the Epitheleal Monolayer

Figure 1 illustrates the effects of increasing concentrations of PA on current, voltage, and resistance. Two separate experiments were performed and the data were normalized to the values of the control condition, 0 mM PA. The effect of PA exhibits a bi-phasic pattern. As the PA concentration increased from 0 to 0.5 mM there was an increase in Isc followed by a marked decrease at concentrations of 1 mM or greater [PA]. Consistent with an increase in Isc, the calculated transepithelial resistance decreased with 0.25 and 0.5 mM PA; however, at higher concentrations of PA we observed a marked drop in resistance. This latter effect, together with the significant decrease in Isc and Vt, strongly suggest that the cells underwent apoptosis. A cardinal feature of apoptosis is fragmentation of DNA, which can be observed by staining nuclei. Figure 2 shows monolayers of A6 cells on filters that were fixed and stained with phalloidin conjugated with Texas red, which specifically binds to polymerized actin, and with DAPI, which stains DNA. The upper panel shows control cells. Phalloidin delineates the peripheral cytoskeleton of cells (chicken-wire pattern). The nuclei are intact. The lower panel shows cells treated with 1 mM PA for 20 h. Polymerized actin is poorly organized, the neat peripheral distribution is lost and clumps of actin appear throughout the field. The nuclei are fragmented and pyknotic. These changes are most consistent with the advanced apoptosis.

Insulin Response in Cells Treated with Palmitic Acid

It has been previously reported that A6 cells respond to insulin by increasing ENaC activity. The values for current and voltage for all PA concentrations were normalized to the control value (0 mM PA). The response to insulin was expressed as the fractional increase after insulin stimulation for each PA concentration. Fig. 3 shows that in control cells (0 mM PA) the Isc increases 100% whereas with increasing concentrations of PA, there is a smaller fractional increase, 46%, 12% and 0% at 0.25, 0.5 and 1.0 mM PA, respectively. The absence of response to insulin with 1 mM is another indication that this concentration of PA is noxious to the cells.

PPARS

The prevalent notion in the literature is that PPARγ agonists, such as Rosiglitazone, stimulate ENaC activity in the distal tubule leading to sodium retention. It is therefore conceivable that the increase in Isc induced by PA, which is an endogenous agonist of PPARs, could be mediated by these receptors. We first verified that PPARα, δ, and γ were expressed in A6 cells. RT-PCR was conducted using RNA extracted from the cells and specific primers for each of the PPAR DNA sequences as seen in figure 4. To test this hypothesis, we treated cells with either Clofibrate, an agonist of PPARα, or Rosiglitazone, an agonist of PPARγ. In previous experiments we showed that in A6 cells ENaC does not respond to these drugs. We next pretreated cells with both 0.5 mM PA and clofibrate or rosiglitazone. Fig. 6 shows there is no statistically-significant difference between the conditions. From these results it is unlikely that PPARs are the mechanism through which PA is inducing ENAC expression.

Western Blot Analysis

ENaC is composed of three subunits *α, β, and μ*. The Western blot, shown in Figure 7, shows an increased signal for each of the subunits at 0.25 mM and 0.5 mM. This trend parallels the pattern seen in Figure 1. Western blot signals are determined by the quantity of the protein present. To verify we had collected a similar amount of cells in each sample we measured the Na/K ATPase protein as well as the actin, both of which should be expressed equally throughout the samples. These results reinforced our earlier observations from the short-circuit current measurements that PA at certain concentrations increases the abundance of ENaC proteins and that at higher concentrations appears to severely damage the cells.

Visualizing the Mononlayer with Oil Red O

When lipids are incorporated into cells there are three possible pathways they enter: 1) they can be oxidized for energy in the mitochondria; 2) they can be conjugated to glycerol and stored as triglycerides; 3) or, they can be incorporated into the membranes as phospholipids. When lipids enter the triglyceride pathway, the lipid is neutralized and stored in droplets within the cell. Not all cells are capable of storing triglycerides in this way. To determine possible mechanisms for cellular damage, we stained the cells with Oil red O (ORO). ORO is used to show droplets of triglycerides stored in cells. Figure 8 shows a staining of A6 cells treated with 1 mM PA. There are no obvious accumulations of triglycerides within the cells and the nuclei are pyknotic, consistent

with apoptosis. The lipids must have entered one of the other two pathways, and caused significant cellular stress.

DISCUSSION

Type 2 diabetes, metabolic syndrome, and dyslipidemias are issues of great concern for the medical and public health communities. In addition to the multiple problems resulting from these diseases hypertension often accompanies them as a dangerous and costly co-morbidity. Although the associations are likely to be multi-factorial, one possible cause of the hypertension could be fluid over-load from chronic ENaC-mediated retention of sodium by the kidneys in response to the elevated insulin found in these states. Additionally elevated serum FFA levels accompany most hyperinsulinemic conditions. It is well known that FFA deposits in tissues such as muscle and liver have been shown to cause insulin resistance in those tissues. TZDs are insulin-sensitizing drugs whose discovery has been a boon to many type 2 diabetics but unfortunately whose use is limited by a side effect of fluid-retention leading to edema and congestive heart failure in up to 15% of patients using them{{227 Mudaliar,S. 2003; }}. In this study we set out to determine if A6 renal cells became resistant to insulin-induced expression of ENaC following exposure to increasing concentrations of FFAs and to determine if TZD-induced fluid retention is the result of distal tubular activation of ENaC.

We exposed monolayers of A6 cells to PA in concentrations of 0, 0.25, 0.5, 1, and 1.5 mM for 20 hours, stimulated the cells with insulin, then measured the transepithelial equivalent short-circuit current. We found that PA had many effects on the renal cells: stimulation, apoptosis, and insulin resistance. Unexpectedly we found that concentrations of 0 to 0.5 mM PA led to a significant increase in baseline current,

implying increased ENaC activity, however, at higher concentrations of PA the current decreased and eventually dropped to 0 implying probable apoptosis. As found in multiple other tissues, stimulation with insulin following PA treatment led to a blunting of the insulin response for all concentrations of PA.

Although there is some debate the general consensus is that high levels of serum FFAs lead to insulin resistance in various tissues {{230 Boden,G. 1997; }}{{231 Roden,M. 1996; }}. The mechanism for this resistance is less well understood. In muscle, insulin activates a tyrosine kinase receptor that leads to tyrosine phosphorylation and, consequently, to the phosphorylation of other cellular substrates such as the insulin receptor substrate-1 (IRS-1). Once phosphorylated IRS-1 can then bind PI-3 kinase which catalyses the proteins necessary for glucose transportation. Reynoso et al found a dramatic decrease in the phosphorylation levels on both the insulin receptor and the IRS-1 in animals treated with PA that could account for the resulting observed insulin resistance{{232 Reynoso,R. 2003; }}. Though the mechanism for insulin resistance may be similar in renal cells there is much ground to cover before that assumption can be made since the pathway for insulin's effects in distal tubule cells has yet to be elucidated.

Sparangna et al demonstrated that cells treated with PA became apoptotic and Belosludtsev et al provided a possible mechanism {{233 Belosludtsev,K. 2006; }}{{234 Sparagna,G.C. 2004; }}. They proposed that PA/Ca++ complexes induced pores in the mitochondrial membrane leading to a drop in mitochondrial membrane potential and ultimately a release of the pro-apoptotic signal cytochrome c. Eitel et al demonstrated

that FFA-induced apoptosis in human β-cells was substantially reduced when a PKC inhibitor (U-713122) was used on the cells, indicating another possible mechanism for FFA-induced apoptosis {{236 Eitel,K. 2003; }}. As with the insulin pathway in renal cells, the mechanism for PA-induced apoptosis in renal cells is an area of new research and may follow similar pathways; and if a similar pathway is demonstrated, inhibitors such as a PKC inhibitor may prove to mitigate damage done to renal cells exposed to high concentrations of PA.

There are many reports of FFAs acting as both intra-cellular signals and as ligands for cell-surface receptors. Briscoe et al. found that medium and long chain fatty acids acted as ligands for G protein-coupled receptors in both the brain and in pancreatic β-cells {{229 Briscoe,C.P. 2003; }} and it is well established that FFAs act as intracellular ligands for PPARs. One teleological argument for FFAs acting as ligands is simply that after ingesting a food-source FFAs would be released into a system and would appear to be the simplest mechanism for up-regulating certain processes. In the case of FFAs acting as agonists for ENaC activity in the distal tubule an argument could be made that in an environment where Na+ is scarce a meal with large amounts of K+ could lead to a dangerous hyperkalemia and a loss of Na+ if the kidneys didn't reabsorb the Na+ while secreting the K+. As stated previously, the principal cells of the distal tubule insert ENaC channels into the apical cell membrane when stimulated. As Na+ rushes into the cell from the lumen it diminishes the electrochemical gradient and, coupled with the steep K+ concentration gradient, K+ is forced into the lumen and excreted with the urine.

We postulated that PA's effect on distal tubule cells could be mediated by activation of PPARs as PA has been shown to be an agonist of these proteins in other tissues. TZDs are a class of drug that, among other actions, increase insulin sensitivity in peripheral tissue by binding to PPARs. Studies have concluded that TZDs can cause fluid retention, edema, and congestive heart failure in up to 15% of patients depending on their other treatment modalities i.e. supplemental insulin injections leads to a higher incidence of fluid retention and associated co-morbidities{{227 Mudaliar,S. 2003; }},{{228 Guan,Y. 2005; }},{{207 King,K.A. 2004; }}. We proposed that ENaC stimulation in distal tubule renal cells following exposure to TZDs could be the cause of the excess fluid retention. There is disagreement in the literature concerning this point with Guan et al showing activation of ENaC channels following TZD treatment and Nofiziger et al unable to reproduce those findings {{205 Nofziger,C. 2005;206 Guan,Y. 2005; }}. In our experiments there was not a correlation between TZD use and increased ENaC activity in A6 renal cells agreeing with the results of Nofiziger et al {{169 Nofziger,C. 2005; }} and implying another mechanism for the observed fluid retention.

In summary, we found that exposure to high-levels of PA increases sodium transport in renal epithelial cells of the distal tubule thereby contributing to the development of HTN; and that levels > 0.5 mM can prove toxic to the same cells. We also found that TZDs did not have an insulin sensitizing effect on ENAC expression in these cells at base line, with insulin, or with exposure to PA.

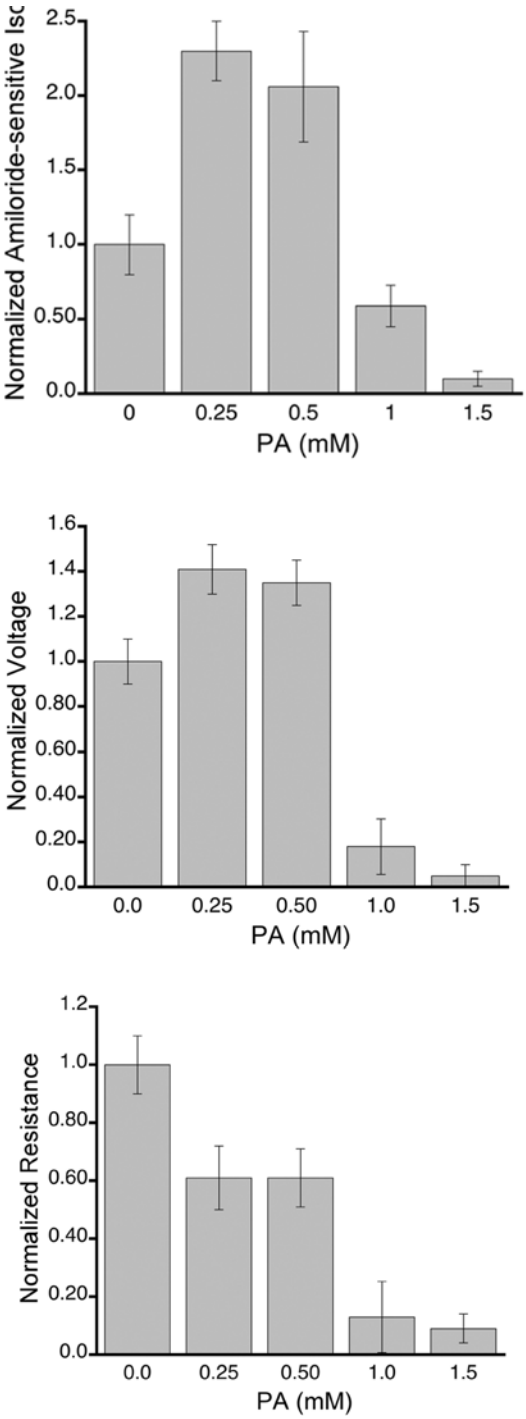

FIGURE 1. *Effects of increasing concentrations of palmitic acid on current, voltage, and resistance in the A6 epithelial monolayer*. A6 cells grown on filters and pretreated with 100 nM of aldosterone were exposed to concentrations from 0 mM – 1.5 mM of PA for twenty hours. Their current, voltage, and resistance were measured using equivalent short-circuit current. Each bar is the mean of two independent experiments normalized to the control.

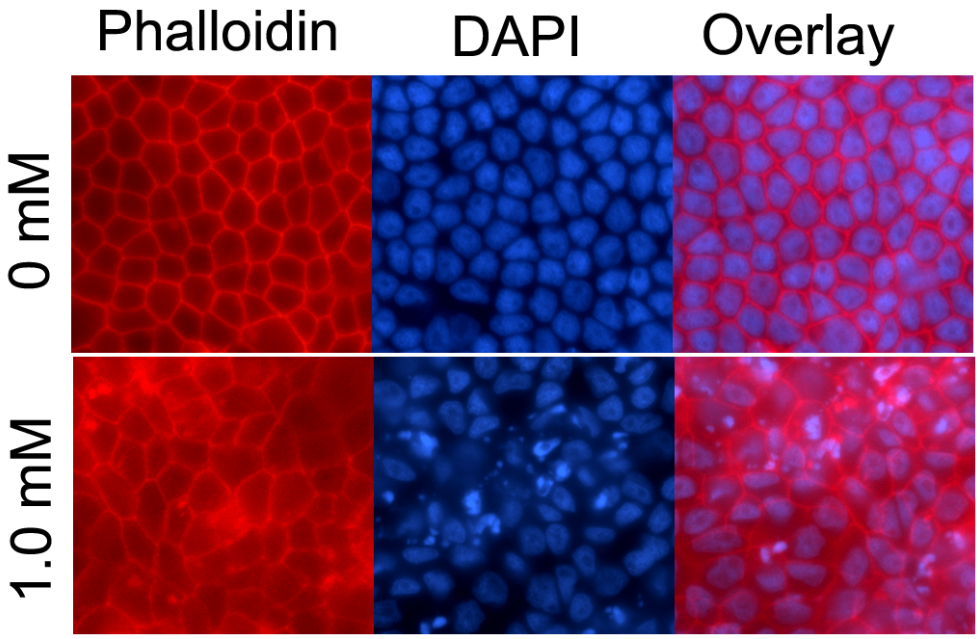

FIGURE 2. *A6 cells stained with phalloidin conjugated with Texas red and DAPI illustrating cellular damage*. Following 20 hours exposure to 1 mM palmitic acid, A6 cells were fixed and stained with phalloidin conjugated with Texas red which binds to polymerized actin and DAPI which stains DNA. The cells were then visualized under fluorescent microscope. The upper panel shows the control cells (0 mM PA). The lower panel shows cells exposed to 1 mM PA. The actin is clearly visualized in the first column as the red staining. The control shows a markedly more organized structure than the 1 mM stain. Similarly the nuclei (blue) in the DAPI stain are robust in the control and pyknotic in the the 1 mM sample.

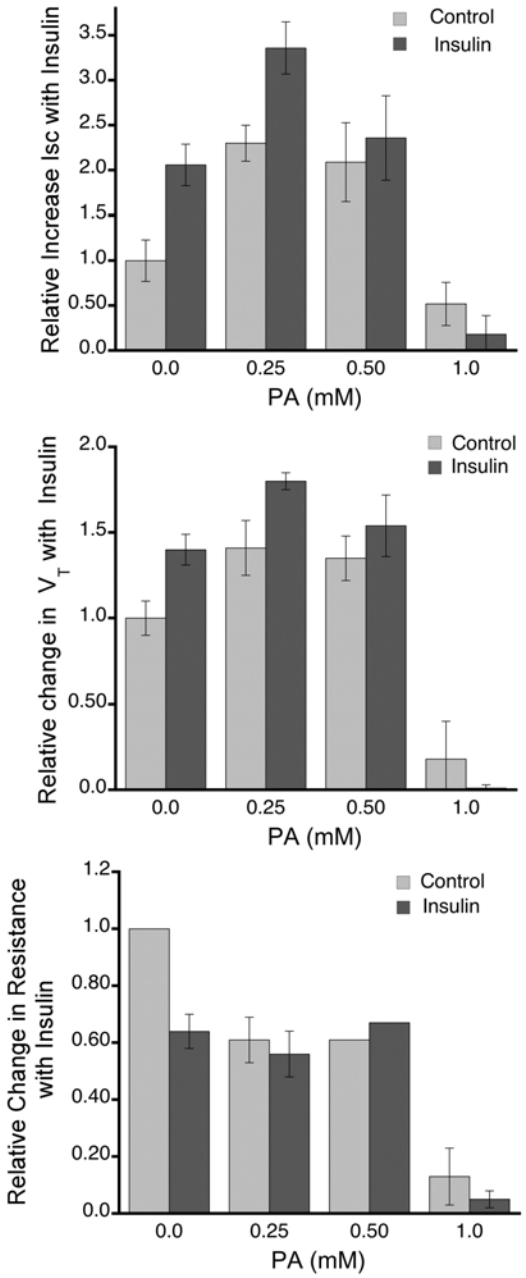

FIGURE 3. *Insulin response in cells treated with Palmitic Acid*. Cells were treated as in Figure 1 after which insulin was added to the cultures and currents and voltages were measured 30 minutes later. The values for all PA concentrations were normalized to the control value (0 mM PA). Each bar is the mean of two independent experiments normalized to the control.

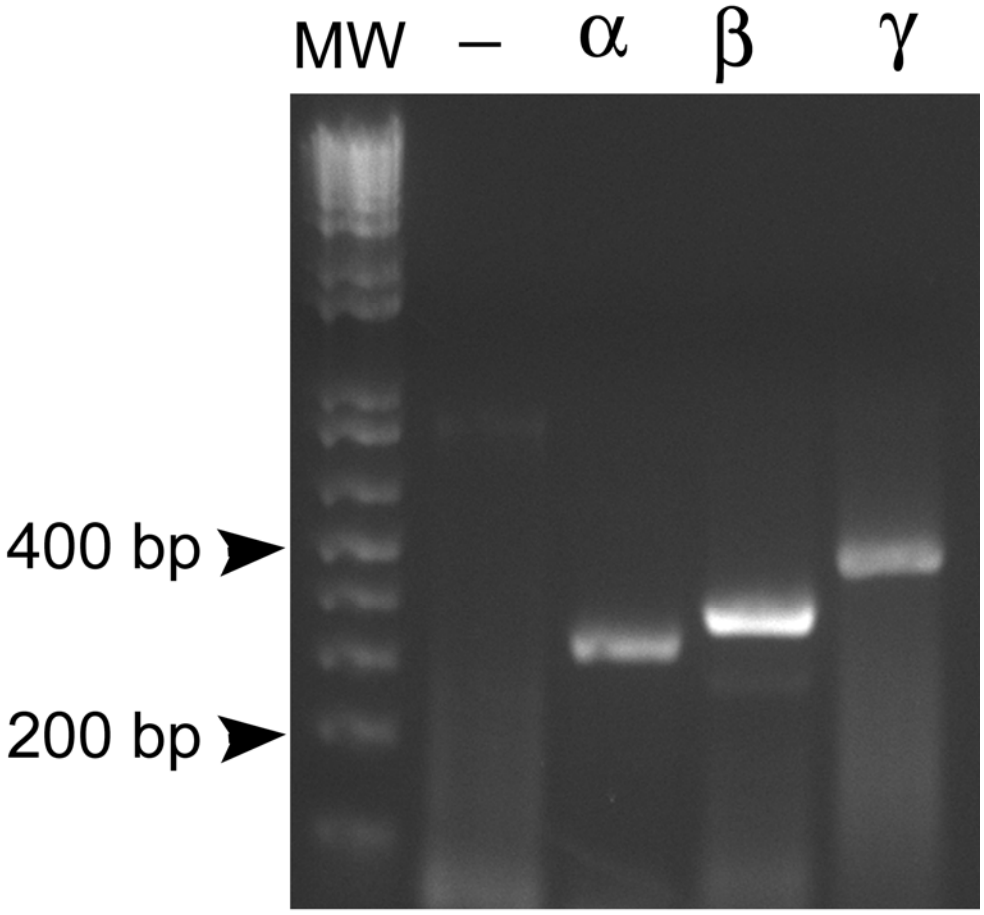

Figure 4. *RT-PCR illustrating the presence of PPARα, PPARδ/β, and PPARγ in A6 cells.* RT-PCR was conducted using RNA extracted from the study cells and specific primers for each of the DNA sequences for PPARα, PPARδ/β, and PPARγ.

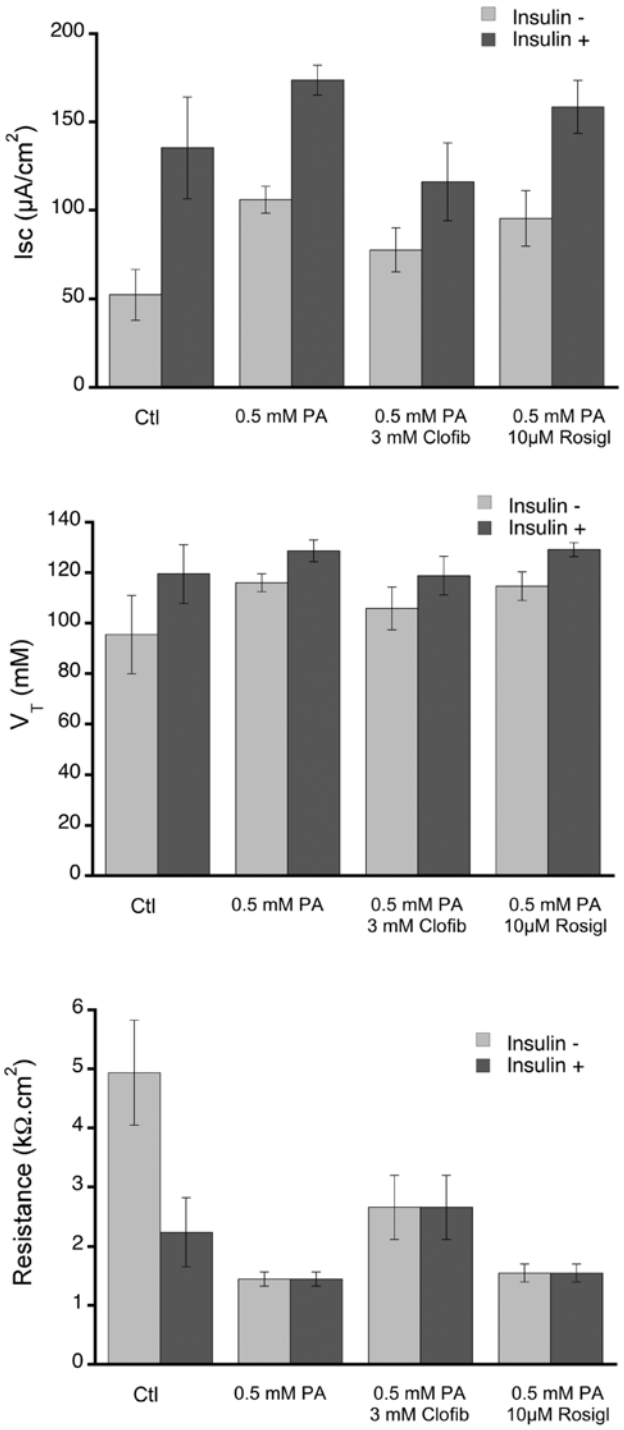

FIGURE 5. *Effects of PPAR agonists on ENaC expression following exposure to 0.5 mM palmitic acid*. A6 cells were treated as in figure 1 in concentrations of 0.5 mM PA and were then exposed to 10 μM of Rosiglitazone (PPARg agonist) or 3 mM of Clofibrate (PPARa agonist). The currents and voltages were measured using short-circuit current and the resistance was calculated using Ohm's law. There was no statistically significant difference between each of the conditions. Each bar is the mean of two independent experiments.

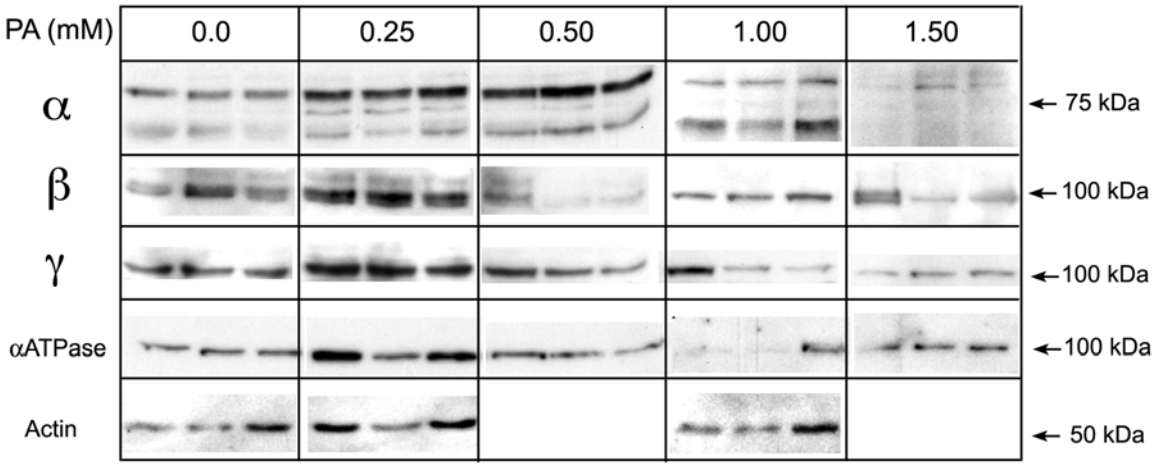

FIGURE 6. *Western blot for ENaC subunits following PA exposure*. A6 cells were solubilized and ENaC subunits were detected by Western blotting with affinity purified anti-xENaC antibodies. Actin was detected with mouse anti-actin antibody. Western blots are shown for each of the three ENaC subunits as well as ATPase and in all five conditions. The actin in the 0.5 and 1.5 mM concentrations could not be collected due to technical difficulty.

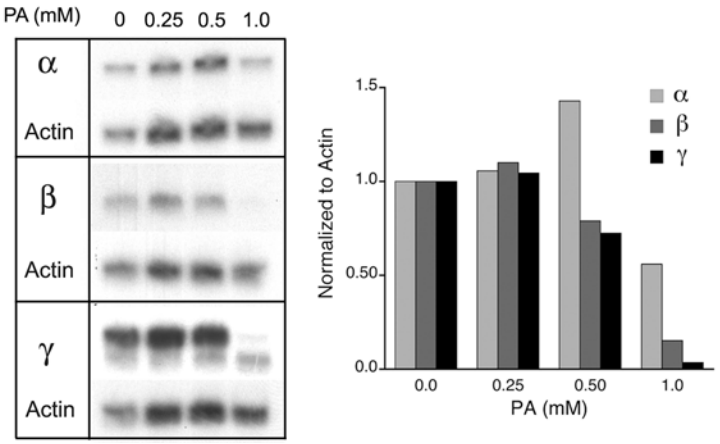

FIGURE 7. Northern blot of ENaC subunits of A6 cells treated with the indicated concentrations of PA. Each blot was hybridized with the corresponding ENaC subunit and actin probes. Graph represents data normalized to actin using a densitometer.

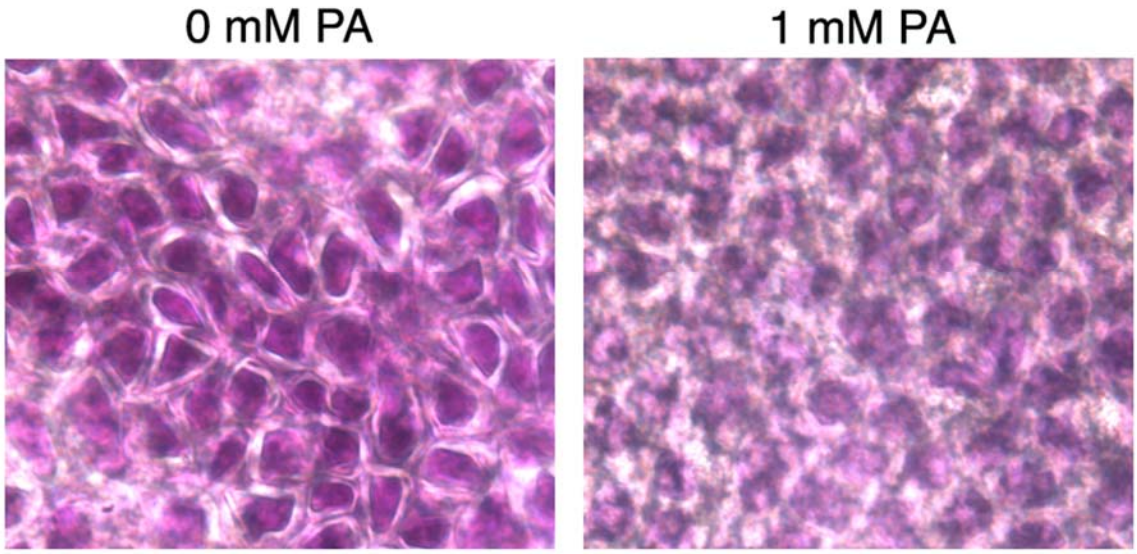

FIGURE 8. *Oil Red O stain for lipid deposits in cells*. A6 cells were treated with 0 mM or 1 mM palmitic acid for 20 hours. The filters were stained with Oil Red O; a fat soluble stain used for staining triglycerides within cells. Filters were also stained with haematoxylin; a stain used for DNA to visualize the nucleus. Despite the background noise of the filter picking up the stains, there are no clear lipid droplets within the cells and the nuclei are pyknotic and damaged in the 1 mM condition.